JOURNAL OF
**Veterinary
Science**

Original Article

Evaluation of a canine small intestinal submucosal xenograft and polypropylene mesh as bioscaffolds in an abdominal full-thickness resection model of growing rats

A-Jin Lee[1], Sung-Ho Lee[1], Wook-Hun Chung[1], Dae-Hyun Kim[1], Dai-Jung Chung[3], Sun Hee Do[2], Hwi-Yool Kim[1,*]

Departments of [1]Veterinary Surgery and [2]Veterinary Clinical Pathology, College of Veterinary Medicine, Konkuk University, Seoul 143-701, Korea
[3]School of Veterinary Medicine, University of California, Davis, CA 95616, USA

We evaluated the biological scaffold properties of canine small intestinal submucosa (SIS) compared to a those of polypropylene mesh in growing rats with full-thickness abdominal defects. SIS is used to repair musculoskeletal tissue while promoting cell migration and supporting tissue regeneration. Polypropylene mesh is a non-resorbable synthetic material that can endure mechanical tension. Canine SIS was obtained from donor German shepherds, and its porous collagen fiber structure was identified using scanning electron microscopy (SEM). A 2.50-cm^2 section of canine SIS (SIS group) or mesh (mesh group) was implanted in Sprague-Dawley rats. At 1, 2, 4, 12, and 24 weeks after surgery, the implants were histopathologically examined and tensile load was tested. One month after surgery, CD68+ macrophage numbers in the SIS group were increased, but the number of CD8+ T cells in this group declined more rapidly than that in rats treated with the mesh. In the SIS group, few adhesions and well-developed autologous abdominal muscle infiltration into the SIS collagen fibers were observed. No significant differences in the tensile load test results were found between the SIS and mesh groups at 24 weeks. Canine SIS may therefore be a suitable replacement for artificial biological scaffolds in small animals.

Keywords: biological scaffold, canine small intestinal submucosa (canine SIS), inflammatory response, polypropylene mesh, tensile load test

Introduction

Abdominal wall defects may develop after traumatic injury, necrotizing infection, tumor resection, congenital defects (*e.g.*, omphalocele), and ventral wall hernias that form after dehiscence of laparotomy wounds. Primary closure of the abdominal wall under tension may promote wound ischemia, thus predisposing patients to dehiscence and evisceration [26]. Reconstructive options that minimize tension include local advancement, the use of flaps and distant flaps, or combined use of flaps and a mesh [17]. Autologous tissue repair can be accomplished by undermining tissues and rotating flaps, but this technique is limited by the defect size and integrity of the abdominal wall [23].

An ideal graft would be biologically safe, secure, able to withstand tensile force, and could grow with the patient, thereby preventing body wall deformity. Previous animal studies have evaluated biologic scaffold materials composed of extracellular matrix (ECM) as alternatives to a synthetic mesh. Small intestinal submucosa (SIS) along with the adjacent connective tissue layer of the mammalian small intestine is comprised of type I collagen fibers [4], glycosaminoglycan, glycoproteins, and proteoglycans [12,20] that form a complex scaffold. In animal models, SIS has been used for constructive remodeling of the urinary bladder [13], body wall [9], esophagus [6], tendons [7], ligaments [15], blood vessels [14], menisci [11], and bone [24]. Secreted, circulating, and ECM-bound growth factors [*e.g.*, transforming growth factor (TGF)-β, epidermal growth factor (EGF), fibroblast growth factor (FGF)-2, and vascular endothelial growth factor (VEGF)] work in concert to regulate cell migration, proliferation, and differentiation throughout the repair process [18,27].

The primary objective of the present study was to evaluate the capacity of canine SIS to act as an appropriate

biological scaffold for the reconstruction and remodeling of graft lesions. The SIS used in this investigation was derived from canines and distinct from porcine-based graphs used in previous studies [4,9,20]. We evaluated the *in vivo* inflammatory responses of the graft recipients and tensile load capacity of the SIS scaffold after implantation in growing rats over an extended period of time. We compared these properties to those of a widely used polypropylene mesh (Prolene). Growth of the animals in this study produced continuous tension load on the implants and permitted assessment of SIS and artificial mesh efficacy.

Materials and Methods

Study design

Fifty 4-week-old female Sprague-Dawley rats (Orient Bio, Korea) weighing approximately 80 g were used in this investigation. The study protocol was approved by the Institutional Animal Care and Use Committee (IACUC) of Konkuk University (Korea). The rats were randomly divided into two groups. One group received Prolene implants (mesh group, n = 25; Ethicon, USA), and the other received canine SIS implants (SIS group, n = 25). Each group was subdivided into five subgroups that were evaluated at different times after the operation (1, 2, 4, 12, and 24 weeks). We performed tensile load tests and histopathological evaluations.

Canine SIS preparation

German shepherds were presented to the Veterinary Medical Teaching Hospital of Konkuk University as part of an animal body donation program. The donated German shepherds were at risk of being euthanized due to disease or other conditions. Dogs with infectious diseases or intestinal problems were excluded. Segments of the jejunum were obtained from the dogs and prepared within 2 h of euthanasia. Canine SIS samples were prepared as previously described under strictly sterile conditions [5]. Resected segments of the jejunum were rinsed with sterile normal saline. Layers of the mucosa, muscularis, and serosa were removed by mechanical abrasion with a number 10 scalpel (Paragon, USA). The thin, whitish SIS samples were thoroughly rinsed in sterile normal saline and 80% ethanol to remove cell degradation products. The samples were stored at 4°C in sterile normal saline containing lincomycin HCl (120 μg/mL; Huons, Korea), vancomycin HCl (50 μg/mL; SSP Pharm., Korea), and cefotoxim (240 μg/mL; Wooridul Pharm., Korea) for 7 days prior to use. Porous structure of the canine SIS collagen fibers was observed by scanning electron microscopy (SEM) using a JSM-6460 microscope (JEOL, USA; Fig. 1).

Surgical procedure

Anesthesia was induced with 3% isoflurane (Choongwae, Korea) in the rat and maintained by mask-delivered inhalation of 1.5% isoflurane in oxygen. A 2.0 × 2.0 cm full-thickness area of total resection was created in the ventral abdominal wall including the abdominal muscles and peritoneum (Fig. 3A). The implant size was adjusted to 2.5 × 2.5 cm so that it extended 0.25 cm beyond the borders of the resected area, and then sutured without tension to the abdominal wall with 4-0 Maxon (Syneture; Covidien, USA) in a simple continuous pattern. The resected area was repaired with canine SIS (SIS group) in one group and Prolene polypropylene mesh in the other (mesh group). The canine SIS grafts were thoroughly rinsed in sterile normal saline and prepared as two-layered SIS sheets. The skin was closed with 4-0 Dafilon (B. Braun, Germany) in a simple interrupted pattern. After surgery, enrofloxacin (Baytril; Bayer, Germany) was administered for 3 days (10 mg/kg, sid, subcutaneous injection).

Clinical examination and necropsy

The rats were euthanized 1, 2, 4, 12, or 24 weeks after implant placement. Each animal was anesthetized with 5% isoflurane in oxygen and then euthanized by an intracardiac injection of potassium chloride (2 mEq/kg). Seroma and hematoma formation was scored on a 3-point scale (1: no formation, 3: significant swelling), and adhesion formation was scored on a 4-point scale (1: no adhesion, 4: dense adhesion). The length and width of the implants were measured to assess changes in implant area relative to changes in the recipient body weight. Each implant was cut in half; one half was used for histopathological evaluation while the other was used to assess thickness and tensile strength of implant.
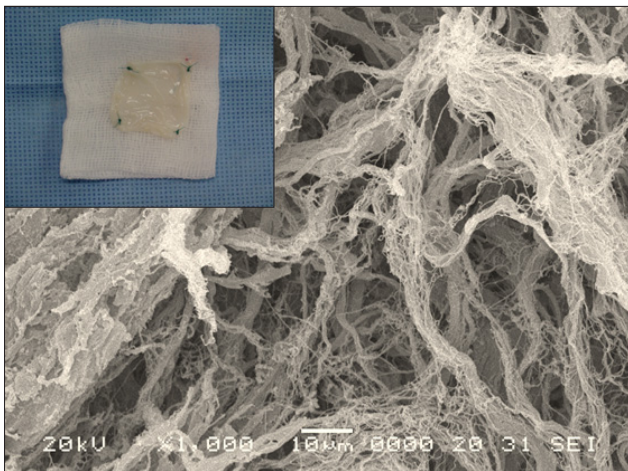

Fig. 1. Photograph of a naïve decellularized canine SIS scaffold (insert) and an SEM image of the SIS surface. Collagen fibers formed an aporous structure.

Histological and immunohistochemical evaluation

Samples were fixed in 10% buffered formalin and embedded in paraffin. The fixed samples were cut into serial 5-μm sagittal sections (microtome AS325; Shandon, USA) and stained with hematoxylin and eosin (H&E; Sigma-Aldrich, USA) to evaluate tissue morphology, Masson's trichrome (Sigma-Aldrich, USA) to observe collagen, and toluidine blue (Sigma-Aldrich, USA) to identify mast cells. The presence of cytotoxic T cells and macrophages was assessed by immunohistochemical (IHC) staining for CD8+ T cells and CD68+ macrophages. The sections were stained with a primary monoclonal rabbit EP 1150Y antibody against CD8 (1 : 250; Abcam, UK) and a primary monoclonal mouse PG-M1 antibody against CD 68 (1 : 100; Dako, USA) at 4°C overnight. The secondary antibodies as biotinylated goat anti-rabbit IgG (Vector Laboratories, USA) at 1 : 200 dilution, and horse anti-mouse IgG (Vector, USA) diluted to 1 : 200 were applied for 30 min at room temperature.

A Vectastain ABC Elite system (Vector Laboratories, USA) and 3,3′-diaminobenzidine system (DAB; Dako, USA) were used to detect antibody binding. The slides were counterstained with Harris hematoxylin (Sigma-Aldrich, USA). The number of positively stained macrophages, cytotoxic T cells, and mast cells were counted in four non-overlapping fields per slide at a magnification of 400× (Leica DM1000, Leica DFC290 HD digital camera; Leica, Germany). These fields were randomly selected along the interface between the implant and surrounding native tissue. The individual who analyzed the slides was blinded to both the study group as well as the interval between surgery and euthanasia.

Measurement of implant thickness and tensile load test

Thickness of the implants was measured five times at selected locations in the central part of the implants using an electronic digital outside micrometer (Schut Geometrical Metrology, the Netherlands). Samples intended for biomechanical testing were packed in cryotubes (Thermo Scientific, USA) immediately after necropsy and stored at $-80°C$. Before testing, the samples were thawed in the cryotubes for 4 h at room temperature. We used a Model 4465 tensiometer (Instron, USA) to test the maximum stress and maximum strain of the samples. The samples were stretched with a crosshead speed of 10 mm/min until they ruptured.

Statistical analyses

All statistical analyses were performed using SPSS (ver. 16.0; IBM, USA). Data for all samples within each group were combined and expressed as the mean ± standard error of the mean (SEM) or SD. Unpaired t-tests or nonparametric Mann-Whitney U tests were used to compare the groups. Kruskal-Wallis tests were used to compare results from the different groups at each time point. P values < 0.05 were considered statistically significant.

Results

Implant thickness and tensile load test results

Mean thickness of the naïve two-layer SIS sheets was 0.80 ± 0.07 mm and that of the naïve synthetic mesh was 0.49 ± 0.02 mm. Mean thickness of the SIS was the greatest (3.07 ± 0.12 mm) 2 weeks after surgery. Mean thickness of
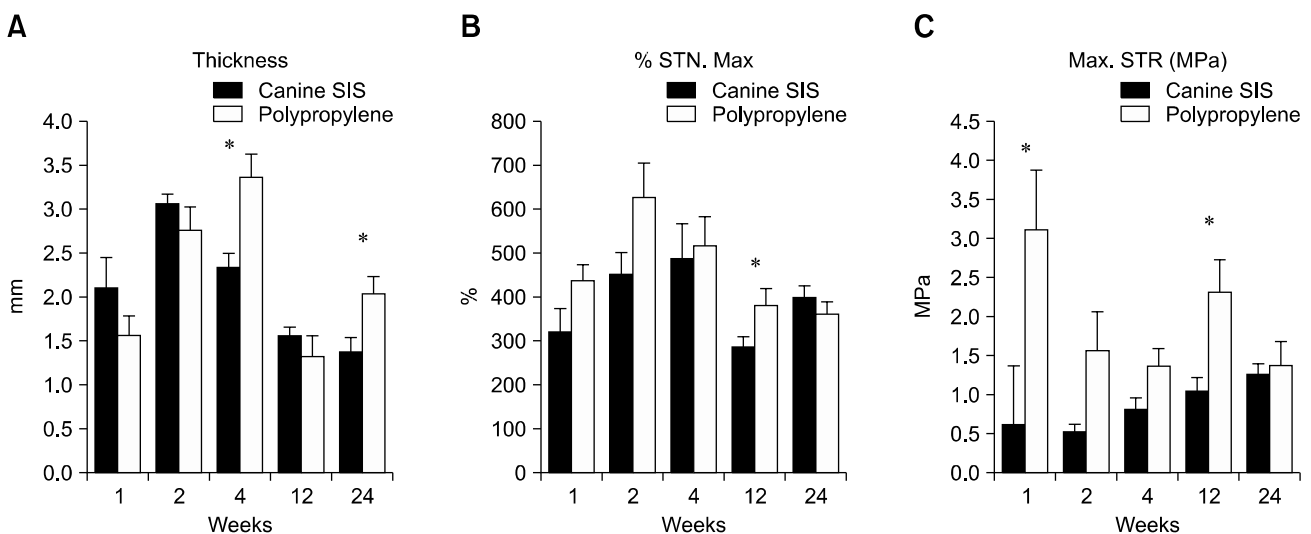

Fig. 2. Results of the tensile load tests for the canine SIS and polypropylene mesh implants. Data are expressed as the mean ± SEM. Asterisks indicate significant differences ($p < 0.05$) in (A) implant thickness (mm), (B) maximum strain (%), and (C) maximum stress (MPa) between the two groups.

the mesh was the greatest (3.36 ± 0.27 mm) 4 weeks after implantation. After 12 weeks, no significant intergroup differences in thickness were observed. However, the synthetic mesh thickness was approximately 1.5-times that of the SIS implant after 24 weeks (mesh = 2.03 ± 0.21 mm; SIS = 1.40 ± 0.16 mm; $p = 0.047$; Fig. 2A).

Mean maximum strain of the naïve SIS sheets measured by the tensile load test was $283.44 \pm 28.95\%$ and that of naïve mesh was $164.40 \pm 30.27\%$. Twelve weeks after implantation, there was a significant intergroup difference in maximum strain ($p = 0.047$) but no significant difference ($p = 0.465$) was found after 24 weeks (SIS = $405.90 \pm 27.05\%$, mesh = $365.68 \pm 29.72\%$; Fig. 2B). Mean maximum stress of the naïve SIS sheets was 2.56 ± 0.36 MPa while that of the naïve mesh was 1.23 ± 0.23 MPa. A

significant difference in maximum stress was observed between the two groups 12 weeks after implantation ($p = 0.016$). Twenty-four weeks after surgery, no significant difference ($p = 0.754$) was found (SIS = 1.29 ± 0.13 MPa, mesh = 1.41 ± 0.24 MPa; Fig. 2C).

Macroscopic findings

All rats displayed normal eating, drinking, urination, and defecation behavior throughout the study. Mean scores for seroma, hematoma, and adhesion development for each group over time are presented in Table 1. In the mesh group, fibrous tissue was partially integrated over the implants, resulting in the formation of seromas or hematomas. There was evidence indicating that the hematomas observed 12 and 24 weeks after surgery

Table 1. Macroscopic evaluation of polypropylene mesh (M) and canine SIS (S) implants

Wk after implantation	Group SIS / Mesh	Body weight (g)	Post-implant area (cm^2)	Seroma formation (G) 1~3	Hematoma formation (G) 1~3	Adhesion formation (G) 1~4
1	S-1	111.4 ± 2.19	3.46 ± 0.20	1.4 ± 0.55	1.2 ± 0.45	1.2 ± 0.45
	M-1	100 ± 0.00	3.46 ± 0.20	1.2 ± 0.45	2.0 ± 1.0	2.8 ± 0.45
2	S-2	174 ± 11.40	$4.85 \pm 0.93^*$	1.4 ± 0.55	$1.6 \pm 0.55^*$	1.2 ± 0.45
	M-2	161 ± 8.94	3.10 ± 0.88	1.4 ± 0.89	1.0 ± 0.00	3.4 ± 0.55
4	S-3	209 ± 12.45	$4.47 \pm 0.73^{**}$	$1.0 \pm 0.00^*$	1.0 ± 0.00	$1.0 \pm 0.00^*$
	M-3	204 ± 17.10	2.45 ± 0.44	1.6 ± 0.55	1.4 ± 0.89	3.0 ± 0.00
12	S-4	284 ± 35.07	$6.75 \pm 0.94^{**}$	1.0 ± 0.00	1.0 ± 0.00	$1.0 \pm 0.00^*$
	M-4	284 ± 15.17	2.38 ± 0.66	1.0 ± 0.00	1.6 ± 0.89	3.8 ± 0.45
24	S-5	310 ± 50	$12.00 \pm 3.98^{**}$	1.0 ± 0.00	1.0 ± 0.00	$1.0 \pm 0.00^*$
	M-5	328 ± 23.87	2.25 ± 0.00	1.0 ± 0.00	1.2 ± 0.55	4.0 ± 0.00

Data are presented as the mean $\pm$ SD. $^*p < 0.05$ and $^{**}p < 0.001$. Results for the mesh versus SIS implants were compared with a Mann-Whitney U test. The scale used to report the extent of adhesion formation was 1: no adhesion, 2: minimal adhesion that could be easily separated, 3: mild adhesion that was more difficult to separate, and 4: dense adhesion that could only be separated with dissection. The extent of seroma/hematoma formation was graded as 1: no formation, 2: encapsulation with fluid located closely adjacent to the implant, and 3: significant swelling.
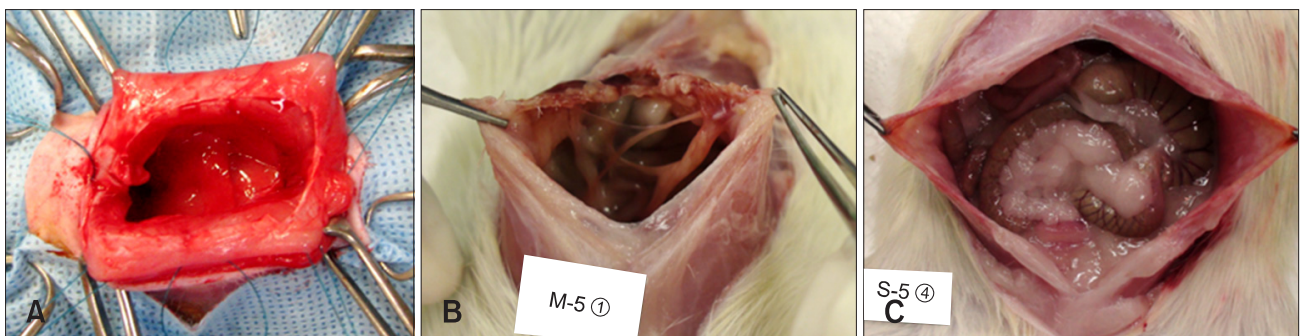

Fig. 3. Photograph of the visceral portion of the polypropylene mesh or canine SIS 24 weeks after implantation. (A) An area (2.0×2.0 cm) of full-thickness total resection (external abdominal oblique, transverse abdominis muscles, and peritoneum) was made in the ventral abdominal wall. (B) In the polypropylene mesh group, adhesions between the intestine or omentum and the mesh were observed along with hematomas. (C) In the canine SIS group, neither adhesion formation nor host muscle infiltration was observed.

resulted from loss of the central implant region. At all time points, the mesh was markedly attached to the broad omentum located around the intestine and liver margin. These lesions became progressively worse over time ($p = 0.03$ at 4 weeks; Fig. 3B). In the SIS group, neither seromas nor hematomas were found after 4 weeks, and there was no apparent adhesion formation or abdominal organ damage at any time point (Fig. 3C).

After a 4-week period of inflammation, new replacement muscle along the SIS implant was observed, particularly in the adjacent abdominal muscle layer. In some rats, the central area of the SIS implant had a translucent appearance after 3 ~ 6 months that could be attributed to a lack of infiltrating muscle fibers. Significant intergroup differences were observed in graft size for periods of time after surgery longer than 2 weeks ($p = 0.023$). The SIS implant expanded gradually after this time, but the mesh

curved along the shape of the abdomen and contracted by as much as 2.25 cm^2 24 weeks after surgery ($p = 0.005$ between the two groups).

Histopathology

We observed loose connective tissue and inflammatory cells around the mesh implant in the mesh group during the first week after surgery. Circular areas of organized connective tissue surrounding the mesh fibers gradually appeared at 4 weeks. After 12 weeks, these areas had increased thickness and large amounts of cellular deposition including mononuclear cells and collagen with new blood vessels (Figs. 4A and B). Adipose connective tissue accumulated near the border of the mesh, and poorly organized fibrous connective tissue was seen around the mesh grafts 12 and 24 weeks following implantation. Masson's trichrome staining revealed necrotic changes in
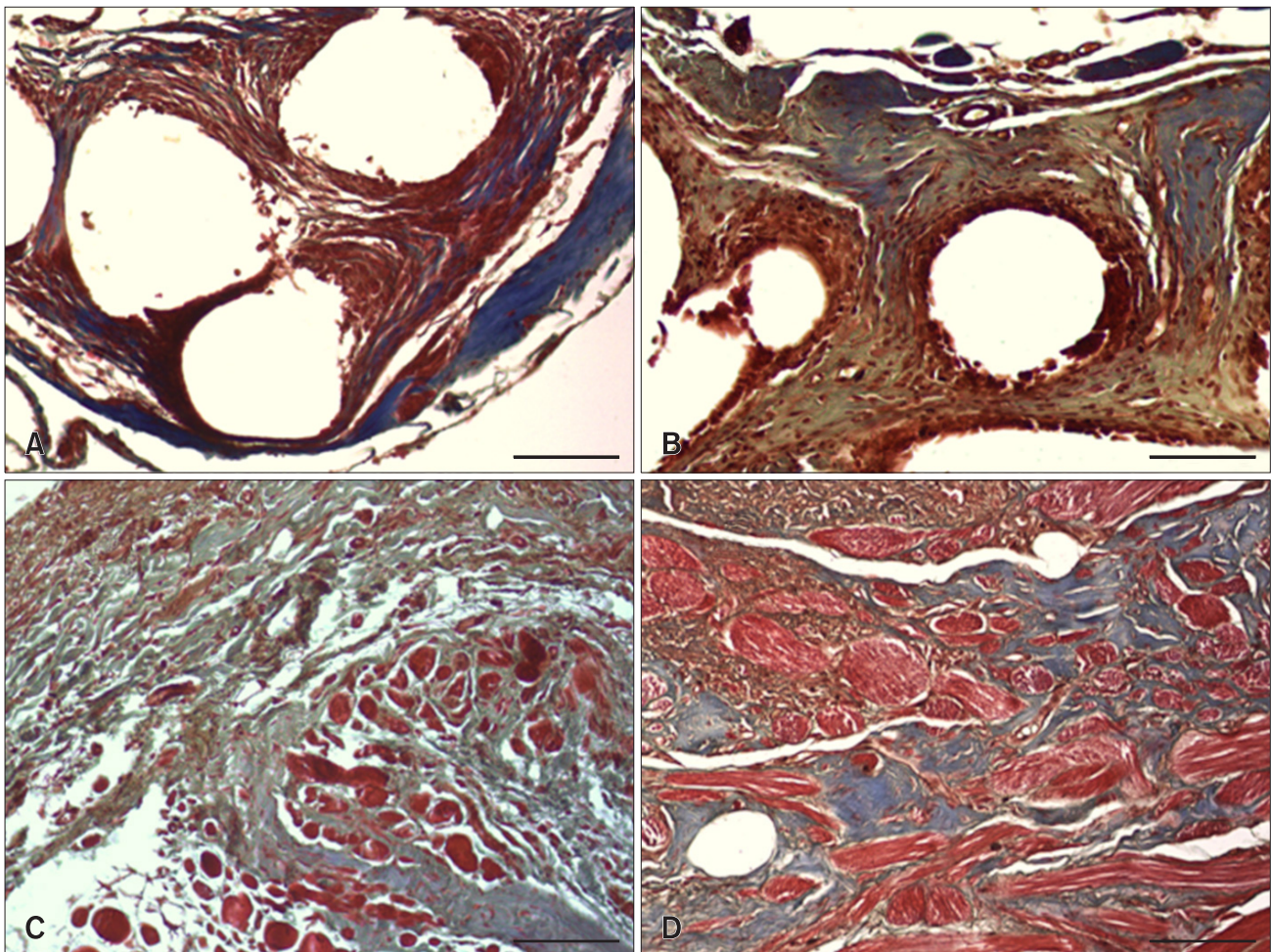

Fig. 4. Masson's trichrome staining for monitoring host tissue morphologic changes (200× magnification). (A) Collagen connective tissue that appeared around polypropylene mesh fibers were identified 4 weeks after surgery. (B) The number of fibroblastic cells appearing around the mesh and collagen increased at 12 weeks. (C) Infiltration of skeletal muscle fibers amid the canine SIS collagen at 4 weeks. (D) The infiltrating muscle fibers developed and were enlarged (red) in the canine SIS implant (blue) by 12 weeks. Scale bars = 100 μm.
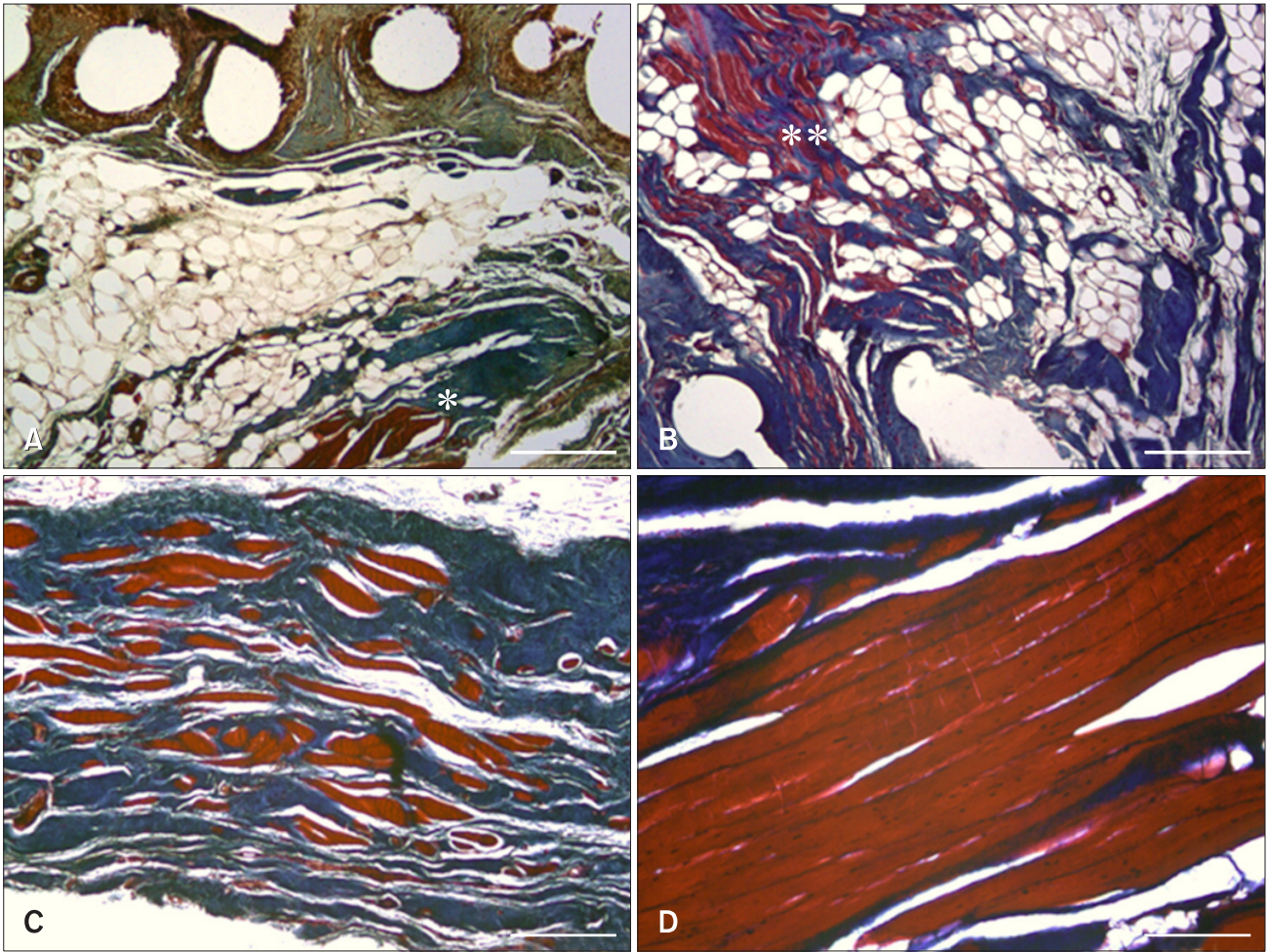
Fig. 5. Masson's trichrome staining for evaluating host tissue responses around the grafts 24 weeks after surgery (100× magnification). (A) Adipose tissue deposited around the mesh and necrotic changes (*) in muscle bundles were identified (B) Accumulation and development of adipose tissue along with weak development (**) of muscle and fibrous connective tissue were observed 24 weeks after surgery in the mesh group. (C) Poorly developed host muscle bundles appeared between the canine SIS collagen fibers (blue). (D) Complete host muscle bundles in the canine SIS implants were identified 24 weeks after surgery. Scale bars = 200 μm.

host muscle bundles (*i.e.*, conversion of red muscle near the mesh into blue collagen), and there was a high level of adipose tissue accumulation around the mesh fibers (Figs. 5A and B).

In the SIS group, the region near the implanted tissue was easily identified with H&E staining by the presence of mononuclear cells and active neovascularization. Four weeks after surgery, the layers of SIS were densely populated with cells that appeared red when stained with Masson's trichrome. These represented areas where newly migrated cells were starting to infiltrate the matrix. Collagen fiber density of the SIS (blue) and muscle infiltration (red) increased gradually into the space immediately surrounding the graft (Figs. 4C and D). At 24 weeks, the SIS collagen had been completely replaced by well-organized skeletal muscle bundles (Fig. 5D). However, we observed poorly developed muscle infiltration in the SIS implants of two rats (Fig. 5C).

Inflammatory cellular responses

Mononuclear cells found in the inflammatory infiltrates around the implants were identified as CD8+- and CD68+-positive cells by IHC staining at each time point (Fig. 6). Mast cells stained with toluidine blue were also found. Mast cell counts revealed that the number of residual cells for the SIS group was highest during the first week after surgery (8.38 ± 2.42). In the mesh group, the mast cells were most numerous at 12 weeks (11.63 ± 2.34). At this time, mast cell counts for the mesh group were approximately 1.8 times greater ($p = 0.032$) than those of the SIS group (SIS = 6.50 ± 0.56, mesh = 11.63 ± 2.34; Fig. 7A). In the SIS group, CD8+ T cells were most numerous at 2 weeks (25.35 ± 5.91) while these cells were most numerous at 4 weeks (37.00 ± 6.97) in the mesh group.
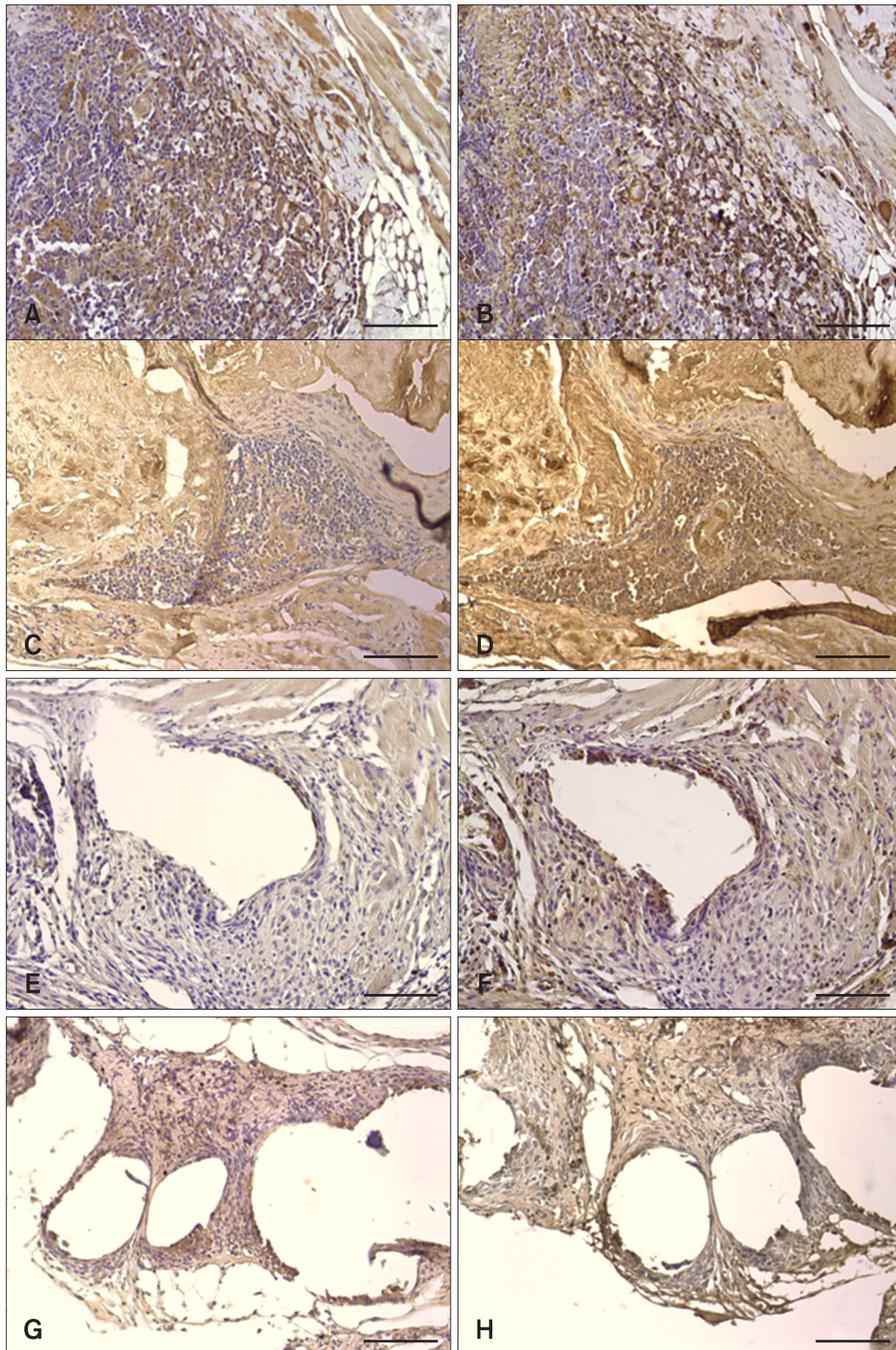
Fig. 6. Immunohistochemical quantification of specific mononuclear cells (CD8+ cytotoxic T lymphocytes and CD68+ macrophages) at 200× magnification. (A) CD8+ T cells in the canine SIS implant 4 weeks after surgery. (B) CD68+ M1 cells in canine SIS at 4 weeks. (C) CD8+ T cells in the canine SIS implant at 12 weeks. Significantly fewer cells were observed at this time compared to 4 weeks. (D) CD68+ M1 cells in canine SIS at 12 weeks. (E) CD8+ T cells around the mesh fibers at 4 weeks. (F) CD68+ M1 cells around the mesh fibers at 4 weeks. (G) CD8+ T cells around the mesh fibers at 12 weeks. (H) CD68+ M1 cells around the mesh fibers at 12 weeks. Scale bars = 100 μm.
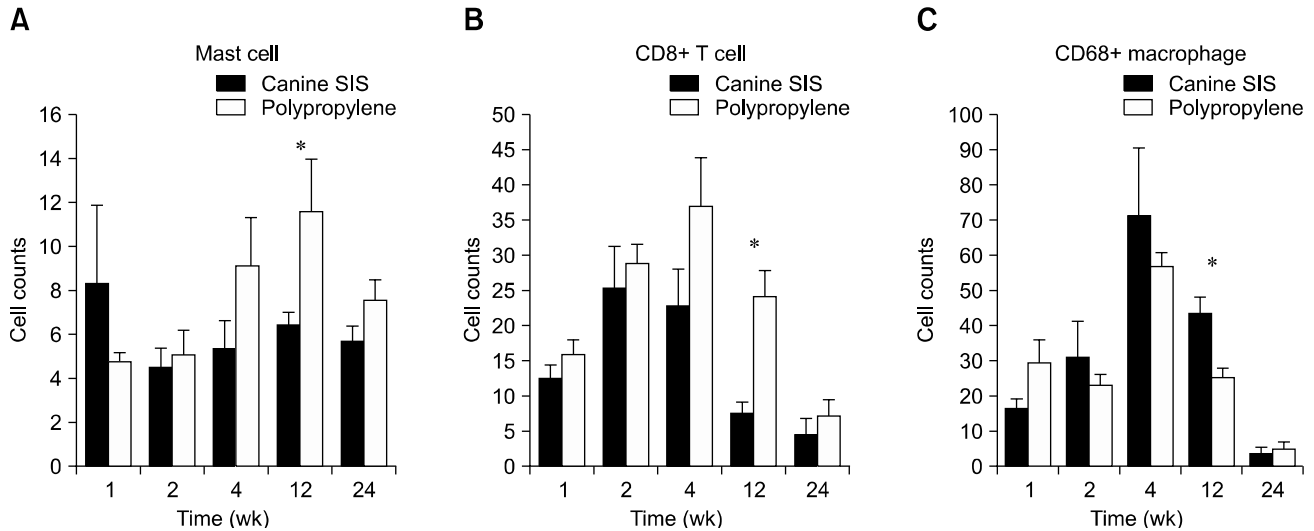
Fig. 7. Inflammatory cell counts for the SIS and mesh groups. Asterisks (*) indicate significant differences ($p < 0.05$) between the canine SIS and polypropylene mesh implants. (A) The number of mast cells for the mesh group gradually increased compared to those of the canine SIS group. (B) The number of CD8+ cytotoxic T cells declined faster in the canine SIS group than in the mesh group. (C) CD 68+ macrophages were more numerous in the canine SIS group than in the mesh group 2 weeks after surgery. At 24 weeks, no significant difference between the two groups was observed.

Twelve weeks after surgery, the CD 8+ T cell count for the mesh group was approximately three times higher ($p = 0.009$) than that of the SIS group (SIS = 7.65 ± 1.63, mesh = 24.25 ± 3.53; Fig. 7B). CD68+ macrophages in both groups were most numerous at 4 weeks (SIS = 71.31 ± 19.52, mesh = 57.20 ± 3.57). Twelve weeks after surgery, the CD68+ cell count of the SIS group was approximately 1.7 times higher ($p = 0.014$) than that of the mesh group (SIS = 43.88 ± 4.00, mesh = 25.45 ± 2.87; Fig. 7C). At 24 weeks, the number of all remaining mononuclear cells was not significantly different between the two groups.

Discussion

In the present study, we focused on identifying differences between the properties of a polypropylene synthetic mesh and canine SIS bioscaffold used for abdominal wall reconstruction in growing rats. Synthetic prosthetic materials such as polypropylene mesh do not grow with the patient when used to repair hernias in young animals. Thus, implants made from these materials can be associated with the formation of restricted body walls movement and recurrent hernias [21].

Macroscopic examination revealed that the mesh generally induced a much greater inflammatory response than canine SIS. The former was associated with abdominal organ adhesions in the intestines, liver margin, and omentum. These adhesions could lead to the development of intestinal obstruction, abdominal organ failure, peritonitis, or pain [3]. The occurrence of hematomas or seromas was evident in the mesh group, and

remnants of these lesions persisted longer in the mesh group than in the SIS group.

We focused on changes in mononuclear cell populations, including mast cells, CD8+ T cells, and CD68+ macrophages, over time. Mast cell responses differed between the SIS and mesh groups. Mast cells persisted for a longer period in the mesh group (until 12 weeks after surgery). These cells can produce an array of both pro- and anti-inflammatory mediators, and express a spectrum of co-stimulatory molecules. Our findings indicate that mast cells play a regulatory role that influences both innate and adaptive immunity [10,16]. Furthermore, mast cells are associated with persistent inflammation and long-term tissue remodeling [10]. Results from the present study suggest that the mesh group had a more persistent inflammatory response than the SIS group.

The CD8+ T cell response in the mesh group persisted for a longer period than in the SIS group with a large number of cells present 4 and 12 weeks after surgery. These cell-mediated immune responses have been previously analyzed by monitoring delayed type hypersensitivity and cytotoxic T cell reactions [2]. Th1 lymphocytes produce cytokines such as interleukin (IL)-2, interferon (INF)-γ, and tumor necrosis factor (TNF)-β responsible for macrophage activation as well as the differentiation of CD8+ T cells into a cytotoxic phenotype [1]. CD8+ T cells have essential roles in the initiation and maintenance of adipose tissue inflammation [19]. Histopathological examination of the immediate vicinity surrounding the mesh grafts revealed extensive deposition of adipose tissue and became weak between muscle fibers and necrotic

changes in host muscle bundles. M1 cells help protect against pathogens by producing high levels of TNF-α, IL-1β, IL-6, and IL-12 along with low levels of IL-10. These cells therefore promote Th1-type immune responses [8,25].

Evaluation of implant tensile load and thickness was based on the inflammatory response and degree of tissue remodeling. The greatest SIS thickness was observed 2 weeks after surgery while the maximum mesh thickness was observed at 4 weeks. This result is probably related to the acute inflammatory phase of wound healing and adhesion formation observed in the mesh group. Moreover, the mesh implants shrank and developed a curved shape. Contraction of the mesh fibers during the scarring process leads to shrinkage of the mesh after implantation *in vivo* [3]. This can cause separation along the graft-tissue interface in growing animals, creating the potential for re-herniation [22]. In contrast, the canine SIS implants showed a smaller change in thickness, but muscle infiltration continued and host muscle bundles developed between the SIS collagen layers. Additionally, collagen fiber density of the SIS implants increased over time as did the tensile load. However, the infiltration of host tissue into the canine SIS implant was relatively delayed in two rats and the implant became enlarged with a few infiltrating muscle fibers. We suspect that in these cases a balance between implant degradation and host tissue regeneration was not achieved.

Compared to the polypropylene mesh, implantation of a canine SIS xenograft resulted in better autologous muscle regeneration, improved remodeling of the adjacent tissues, and fewer inflammatory responses. Tensile load test results did not significantly differ between the groups 6 months after surgery. Our results demonstrated that canine SIS could be a new biomaterial scaffold appropriate for clinical practice. However, factors related to bioscaffold degradation and the rate of host tissue replacement suggest that a balance between these events is necessary for functional tissue reconstruction. Therefore, further studies are needed to better understand the various mechanisms underlying biomaterial remodeling in the host and to correlate these findings with eventual clinical outcomes.

Acknowledgments

References

1. **Abbas AK, Murphy KM, Sher A.** Functional diversity of helper T lymphocytes. Nature 1996, **383**, 787-793.
2. **Allman AJ, McPherson TB, Merrill LC, Badylak SF, Metzger DW.** The Th2-restricted immune response to xenogeneic small intestinal submucosa does not influence systemic protective immunity to viral and bacterial pathogens. Tissue Eng 2002, **8**, 53-62.
3. **Amid PK.** Classification of biomaterials and their related complications in abdominal wall hernia surgery. Hernia 1997, **1**, 15-21.
4. **Badylak SF.** Small intestinal submucosa (SIS): a biomaterial conducive to smart tissue remodeling. In: Bell E (ed.). Tissue engineering: current perspectives. 1st ed. pp.179-189, Birkhäuser, Boston, 1993.
5. **Badylak SF, Lantz GC, Coffey A, Geddes LA.** Small intestinal submucosa as a large diameter vascular graft in the dog. J Surg Res 1989, **47**, 74-80.
6. **Badylak S, Meurling S, Chen M, Spievack A, Simmons-Byrd A.** Resorbable bioscaffold for esophageal repair in a dog model. J Pediatr Surg 2000, **35**, 1097-1103.
7. **Badylak SF, Tullius R, Kokini K, Shelbourne KD, Klootwyk T, Voytik SL, Kraine MR, Simmons C.** The use of xenogeneic small intestinal submucosa as a biomaterial for Achilles tendon repair in a dog model. J Biomed Mater Res 1995, **29**, 977-985.
8. **Bystrom J, Evans I, Newson J, Stables M, Toor I, Van Rooijen N, Crawford M, Colville-Nash P, Farrow S, Gilroy DW.** Resolution-phase macrophages possess a unique inflammatory phenotype that is controlled by cAMP. Blood 2008, **112**, 4117-4127.
9. **Clarke KM, Lantz GC, Salisbury SK, Badylak SF, Hiles MC, Voytik SL.** Intestine submucosa and polypropylene mesh for abdominal wall repair in dogs. J Surg Res 1996, **60**, 107-114.
10. **Galli SJ, Nakae S, Tsai M.** Mast cells in the development of adaptive immune responses. Nat Immunol 2005, **6**, 135-142.
11. **Gastel JA, Muirhead WR, Lifrak JT, Fadale PD, Hulstyn MJ, Labrador DP.** Meniscal tissue regeneration using a collagenous biomaterial derived from porcine small intestine submucosa. Arthroscopy 2001, **17**, 151-159.
12. **Hodde JP, Badylak SF, Brightman AO, Voytik-Harbin SL.** Glycosaminoglycan content of small intestinal submucosa: a bioscaffold for tissue replacement. Tissue Eng 1996, **2**, 209-217.
13. **Kropp BP, Eppley BL, Prevel CD, Rippy MK, Harruff RC, Badylak SF, Adams MC, Rink RC, Keating MA.** Experimental assessment of small intestinal submucosa as a bladder wall substitute. Urology 1995, **46**, 396-400.
14. **Lantz GC, Badylak SF, Hiles MC, Coffey AC, Geddes LA, Kokini K, Sandusky GE, Morff RJ.** Small intestinal submucosa as a vascular graft: a review. J Invest Surg 1993, **6**, 297-310.
15. **Liang R, Woo SLY, Takakura Y, Moon DK, Jia F, Abramowitch SD.** Long-term effects of porcine small intestine submucosa on the healing of medial collateral ligament: A functional tissue engineering study. J Orthop Res 2006, **24**, 811-819.
16. **Lu LF, Lind EF, Gondek DC, Bennett KA, Gleeson MW, Pino-Lagos K, Scott ZA, Coyle AJ, Reed JL, Van Snick J, Strom TB, Zheng XX, Noelle RJ.** Mast cells are essential

intermediaries in regulatory T-cell tolerance. Nature 2006, **442**, 997-1002.

17. **Mathes SJ, Steinwald PM, Foster RD, Hoffman WY, Anthony JP.** Complex abdominal wall reconstruction: a comparison of flap and mesh closure. Ann Surg 2000, **232**, 586-596.

18. **McDevitt CA, Wildey GM, Cutrone RM.** Transforming growth factor-β1 in a sterilized tissue derived from the pig small intestine submucosa. J Biomed Mater Res A 2003, **67**, 637-640.

19. **Nishimura S, Manabe I, Nagasaki M, Eto K, Yamashita H, Ohsugi M, Otsu M, Hara K, Ueki K, Sugiura S, Yoshimura K, Kadowaki T, Nagai R.** CD8+ effector T cells contribute to macrophage recruitment and adipose tissue inflammation in obesity. Nat Med 2009, **15**, 914-920.

20. **Pu LL.** Small intestinal submucosa (Surgisis) as a bioactive prosthetic material for repair of abdominal wall fascial defect. Plast Reconstr Surg 2005, **115**, 2127-2131.

21. **Sandoval JA, Lou D, Engum SA, Fisher LM, Bouchard CM, Davis MM, Grosfeld JL.** The whole truth: comparative analysis of diaphragmatic hernia repair using 4-ply vs 8-ply small intestinal submucosa in a growing animal model. J Pediatr Surg 2006, **41**, 518-523.

22. **Smith MJ, Paran TS, Quinn F, Corbally MT.** The SIS extracellular matrix scaffold-preliminary results of use in congenital diaphragmatic hernia (CDH) repair. Pediatr Surg Int 2004, **20**, 859-862.

23. **Smith RS.** The use of prosthetic materials in the repair of hernias. Surg Clin North Am 1971, **51**, 1387-1399.

24. **Suckow M, Voytik-Harbin SL, Terril LA, Badylak SF.** Enhanced bone regeneration using porcine small intestinal submucosa. J Invest Surg 1999, **12**, 277-287.

25. **Verreck FAW, De Boer T, Langenberg DML, Hoeve MA, Kramer M, Vaisberg E, Kastelein R, Kolk A, De Waal-Malefyt R, Ottenhoff THM.** Human IL-23-producing type 1 macrophages promote but IL-10-producing type 2 macrophages subvert immunity to (myco) bacteria. Proc Natl Acad Sci U S A 2004, **101**, 4560-4565.

26. **Voyles CR, Richardson JD, Bland KI, Tobin GR, Flint LM, Polk HC Jr.** Emergency abdominal wall reconstruction with polypropylene mesh: short-term benefits versus long-term complications. Ann Surg 1981, **194**, 219-223.

27. **Voytik-Harbin SL, Brightman AO, Kraine MR, Waisner B, Badylak SF.** Identification of extractable growth factors from small intestinal submucosa. J Cell Biochem 1997, **67**, 478-491.